

## Sustainable and Reusable Gelatin-Based Hydrogel “Jelly Ice Cubes” as Food Coolant. II: Ideal Freeze–Thaw Conditions

Jiahan Zou, Luxin Wang, and Gang Sun\*

Cite This: *ACS Sustainable Chem. Eng.* 2021, 9, 15365–15374

Read Online

ACCESS |



Metrics &amp; More



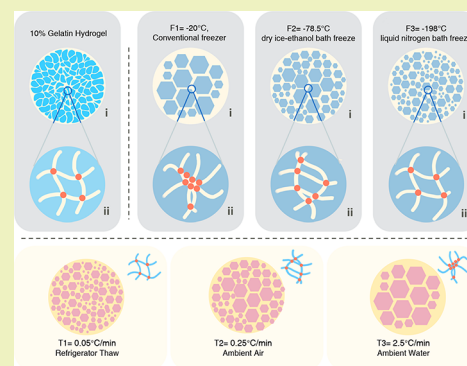
Article Recommendations



Supporting Information

**ABSTRACT:** In an earlier study, jelly ice cubes (JICs) based on 10% gelatin hydrogels were demonstrated as a new type of food coolant. One of the practical challenges associated with the use of JICs was the structural instability against temperature variations during the phase changes of water in hydrogels, which was closely associated with freeze–thaw (FT) conditions. Here, a systematic study on various freezing and thawing rates applied to JICs was conducted to explore the ideal manufacturing and application conditions. Three freezing conditions,  $-20\text{ }^{\circ}\text{C}$  (F1),  $-78.5\text{ }^{\circ}\text{C}$  (F2), and  $-198\text{ }^{\circ}\text{C}$  (F3), and three thawing rates,  $0.05\text{ }^{\circ}\text{C}/\text{min}$  (T1),  $0.25\text{ }^{\circ}\text{C}/\text{min}$  (T2), and  $2.5\text{ }^{\circ}\text{C}/\text{min}$  (T3), were applied with repeated freeze–thaw cycles (FT cycles) to observe the changes of JICs in the latent heat of fusion, water content, mechanical properties, cooling efficiencies, and hydrogel inner structures. The JICs treated with the selected conditions showed significantly improved stability in water content, structural uniformity, heat-absorbing abilities, and lifecycles. With specified FT conditions, the cooling efficiency of JICs remained stable after at least 10 FT cycles. It is anticipated that both the rapid freezing rate and the slow thawing rate assist the formation of uniform polymer networks under repeated freeze–thaw cycles.

**KEYWORDS:** Freezable water, Latent heat of fusion, Mechanical strength, Ice grains in cryogels, Microstructure of cryogels



## INTRODUCTION

Reduction of food loss and waste is one of the global challenges in enhancing food security and environmental sustainability.<sup>1–4</sup> During the preservations of perishable food, temperature abuse falling in the range  $4.4\text{--}60\text{ }^{\circ}\text{C}$  is one of the critical reasons that jeopardizes food safety and quality.<sup>5–7</sup> Traditional ice is extensively used as a food cooling medium in food supply chains due to its high latent heat of fusion near  $0\text{ }^{\circ}\text{C}$ . However, concerns arise on microbial cross-contamination resulting from ice meltwater.<sup>8</sup> As potential replacements, ice packs and new types of antimicrobial ice have been developed and studied.<sup>9–12</sup> Despite the efforts, there is still a vacancy for an ideal food coolant that can comprehensively feature high cooling efficiency, no meltwater, sustainability, reusability, biodegradability, biocompatibility, safety, and zero plastics. Thus, studies in the field are urgently needed.

In the previous study, “jelly ice cubes” (JICs) based on 10% gelatin hydrogels were proposed and tested as a new type of sustainable, reusable, and biodegradable food cooling media that could effectively prevent bacterial cross-contamination by constraining the cooling water component within the hydrogel structures with zero-plastic components.<sup>8</sup> Nevertheless, two critical challenges remained to be solved for the improved practicality of JICs in food cooling applications. First, to achieve the features of reusability, the thermal properties of JICs need to be stable throughout multiple freeze–thaw cycles

(FT cycles, FTCs) with minimum depression in the heat-absorbing abilities. Second, hydrogel systems with robust mechanical properties should be built to achieve minimal structural damage and material flaws during the repeated phase changes of water in the hydrogels through FT cycles. To build a robust system, the degree of physical and chemical cross-linking of gel polymers should be well-controlled. It is of great importance to study the impact of preparation and practical cryogenic conditions on the structures, properties, and functions of JICs to optimize the stability of JICs.

Hydrogels are polymer matrix-supported networks filled with water molecules. When hydrogels go through repeated cycles of freezing, freezing storage, and thawing, they are also referred to as cryogels.<sup>13–15</sup> Based on the interactions with protein polymers, water molecules in the hydrogel are divided into three categories: free water, freezable bound water, and nonfreezable bound water. Upon freezing, the phase change of freezable water, including free water and freezable bound water, induces potential disruptions or damages to the

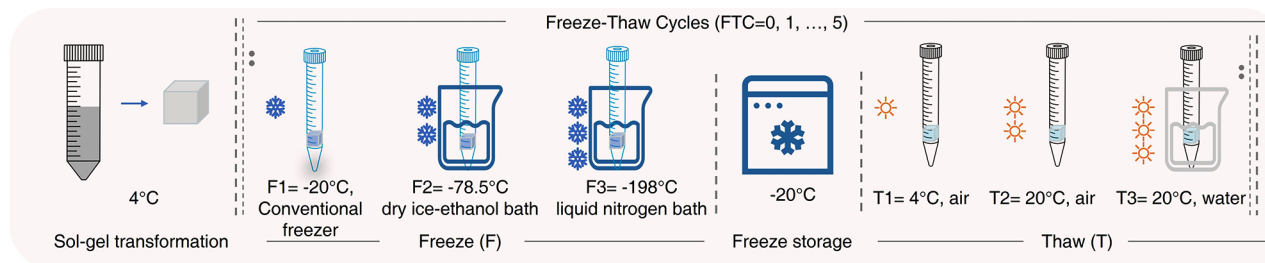
**Received:** September 14, 2021

**Revised:** October 24, 2021

**Published:** November 8, 2021



Scheme 1. Freeze–Thaw Treatments Applied to the JICs to Mimic the Possible Cryogenic and Application Conditions



polymeric structures through the uncontrollable growth of ice grains. A critical factor of controlling the impact of the freeze–thaw process on the polymer network structures is to master the shape and size of the formed ice grains during freezing. The freezing rate of water determines the ice crystal size by changing the nucleation rate.<sup>16</sup> Inspired by the freeze-casting technique in materials science and flash-freezing in food engineering, rapid freezing conditions can potentially be applied to the preparation of JICs to minimize the size of formed ice grains as well as the destructive impact of the phase change of water on the polymer matrix structures.<sup>17,18</sup> In food engineering, similar situations have been extensively studied. Fresh meat and seafood, similar to hydrogels, have 60–80% water in their structures.<sup>17,19–25</sup> The storage condition of meat and seafood is also optimized to retain the desired food qualities. In materials science, studies on the effect of ice-crystals on various systems were conducted.<sup>14,18,26–32</sup> Ice-templating was widely used to develop various organic and inorganic materials with macro-, micro-, and mesoporosity by adjusting the relationship between the ice-fronting velocity and the critical velocity through varying chemical compositions of the systems and the freezing conditions.<sup>18</sup> Many studies reported the effect of controlling freezing rate and pressure on the structure and function of the resulting materials, especially aerogels. However, there is a lack of comprehensive studies that can guide the fabrication and application of JICs by discussing the effect of freezing and thawing conditions on the microstructures of cryogels, specifically on the relationship between the resulting structures to the freezable water content, heat-absorbing ability, and the mechanical properties.

In this study, in order to find the optimized manufacturing and application conditions, JICs based on 10% gelatin hydrogels were prepared and tested for various properties against three levels of freezing rates and three levels of thawing rates. Flash-freezing conditions provided by a dry ice–ethanol bath or a liquid nitrogen bath were employed to find the ideal fabrication and application conditions for JICs.

## MATERIALS AND METHODS

**Materials.** Gelatin (Type A, 225 bloom food-grade) was purchased from MP Biomedicals, LLC (Solon, OH). Poly(vinyl alcohol) (PVA,  $M_n$  85 000–146 000, 99+, hydrolyzed) and ethyl alcohol (pure, 200 proof) were purchased from Sigma-Aldrich (Milwaukee, WI). Riboflavin 5'-phosphate sodium (dihydrate, RBPS) was purchased from Spectrum Chemical (Gardena, CA). Deionized (DI) water was used to prepare the gelatin solutions. Liquid nitrogen and dry ice were used to prepare the freezing bath.

**JICs Preparation and Repeated Freeze–Thaw Treatments.** Homogeneous 10 wt % gelatin solutions were prepared by dissolving gelatin (type A, 225 bloom food-grade, MP) in deionized water at 70 °C and settled in silicon molds (10 × 10 × 10 mm, unless specified)

overnight at 4 °C to complete the gelation. The prepared hydrogels were called JICs at FTC0 before any further FT treatments.

Freeze–thaw methods were applied to the prepared gelatin hydrogels to mimic their multiple freeze–thaw cycles under different conditions. The detailed conditions of multiple FT treatments are shown in Scheme 1. Each FT cycle consisted of initial freezing at various temperatures (freeze until the core temperature of JICs reached F1, F2, or F3), 18 h of storage at –20 °C, and 8 h of thawing at various rates (T1, T2, or T3), sequentially. Various freezing temperatures and thawing rates were F1 = –20 °C, F2 = –78.5 °C, and F3 = –196 °C, representing three levels of possible cryogenic conditions in practice, and T1 (thawed in a 4 °C refrigerator, air; 0.05 °C/min), T2 (thawed in 21 °C, air; 0.25 °C/min), and T3 (thawed in 21 °C, water bath; 2.5 °C/min), simulating three possible application conditions of JICs in a refrigerator, in the air under ambient conditions, or immersed in water at room temperature. Multiple freeze–thaw cycles (C1–C10) were also performed to mimic the repeated usage cycles. Samples were either tested directly or stored at 4 °C after treatments and subjected to ambient conditions before characterizations.

**Characterizations of JICs.** The heat absorbed by the phase change of the freezable water in JICs was tested using a differential scanning calorimeter (DSC-60, Shimadzu Corporation, Pleasanton, CA). The heat-absorbing profiles of JICs were obtained in the temperature range from –30 to 10 °C with a 1 °C/min heating rate under a 50 mL/min protective nitrogen flow. The latent heat of fusion around 0 °C was calculated by integrating the heat flow (W/g)–time (s) curve.

The total water content was tested using a thermal gravimetric analyzer (TGA, SDT-Q600, TA Instrument, New Castle, DE) from ambient temperature to 150 °C with a 10 °C/min heating rate under nitrogen protection. The total water loss was calculated according to eq 1, and the freezable water content was calculated according to eq 2, where  $w$  is the weight of JICs at 110 °C,  $w_0$  is the initial weight of JICs in TGA tests, and  $H$  is the fusion heat of JICs at the specific FT cycle.

$$\text{Total water content (\%)} = \frac{w_0 - w}{w_0} \times 100\% \quad (1)$$

$$\text{Freezable water content (\%)} = \left( \frac{H}{334.5} \right) \div \left( \frac{w_0 - w}{w_0} \right) \times 100\% \quad (2)$$

The testing method for obtaining cooling curves was described in detail by Zou et al.<sup>8</sup> Briefly, the designed device fabricated with Styrofoam was used to provide a stable and isolated environment. Large JICs of 30 × 30 × 20 mm were prepared and conditioned at –20 °C for the test. Large PVA (15%) hydrogels (30 × 30 × 20 mm) photo-cross-linked with 0.5% RBPS and conditioned at 20 °C were used as the cooled objects and placed on top of the JICs. A thermocouple (type K, Omega Engineering Inc., Stamford, CT) with a 4-channel hand-held data logger (Omega Engineering Inc., Stamford, CT) was attached to the top surface's central point of the cooled object to record temperature changes from the moment the object touched the coolant.

The static compressive properties of JICs were obtained using an Instron 5566 tester (Norwood, MA). Static loading cells of 5 kN and

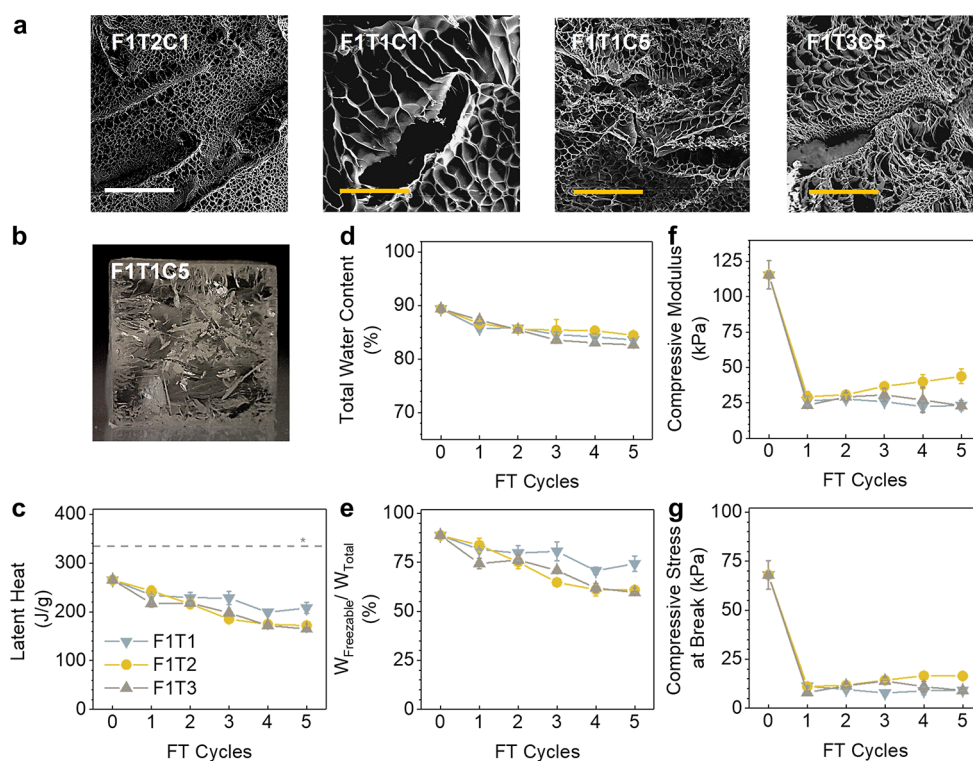


**Figure 1.** (a) SEM images of the lyophilized F1 JICs, with a white scale bar of 500  $\mu\text{m}$  and a yellow scale bar of 100  $\mu\text{m}$ . (b) Photo of the cross-section of an F1 JIC (F1T1C5). (c) Latent heat of the JICs treated under multiple F1TCs. The dashed line with a star symbol represents the latent heat value of traditional ice. (d) Changes of total water content of F1 JICs along multiple F1TCs. (e) Freezable water to total water ratios in the F1 JICs. Static compressive modulus at break (f) and stress at break (g) of the prepared F1 JICs. Plotted data are expressed as means  $\pm$  SD of three replicates.

10 N were used with a compressive rate of 1 mm/min. JIC samples with a size of 10  $\times$  10  $\times$  10 mm were tested for their compressive stress and strain at the breakage point, and the compressive modulus at break was calculated accordingly.

The cross-section of JICs, sliced with disposable feather scalpels (Feather Safety Razor Co., Ltd.), was observed using a Dino-Lite digital microscope (Dunwell Tech. Inc., Torrance, CA). Specimens for SEM images were sliced into small pieces, frozen at  $-198$   $^{\circ}\text{C}$ , and lyophilized by a benchtop K lyophilizer (VirTis, Los Angeles, CA). The internal microscopic structures of lyophilized JICs were observed using a Quattro environmental scanning electron microscope (ESEM, Thermo Fisher Scientific) after being coated with a thin layer of gold (around 8 nm).

**Statistical Methods.** Statistical analyses were conducted using a one-way analysis of variance (ANOVA). All experiments were performed at least three times, and the results are presented as mean value  $\pm$  standard deviation.

## RESULTS AND DISCUSSION

In order to find the best freeze–thaw conditions for the fabrications and applications, freezing temperatures, thawing rates, and cycles of FT treatments and their impact on the related properties and function of JICs were systematically studied. Three levels of cryogenic conditions were employed to discuss the impact of the freezing temperatures (F1 =  $-20$   $^{\circ}\text{C}$ , F2 =  $-78.5$   $^{\circ}\text{C}$ , and F3 =  $-198$   $^{\circ}\text{C}$ ), and three thawing rates (T1 = 0.05  $^{\circ}\text{C}/\text{min}$ , T2 = 0.25  $^{\circ}\text{C}/\text{min}$ , and T3 = 2.5  $^{\circ}\text{C}/\text{min}$ ) corresponding to each freezing condition were investigated, respectively. Up to 10 FT cycles were applied to the JICs to maximize the effect of various FT conditions. In all following discussions, JICs with no FT treatment are treated as the reference specimen, referred to as the FTC0 gels.

### JICs Prepared in a Conventional Freezer (F1 JICs).

JICs were first tested for repeated freezing cycles at  $-20$   $^{\circ}\text{C}$  (F1) and thawed at various rates (T1, T2, and T3). The freezing condition provided by a conventional freezer at  $-20$   $^{\circ}\text{C}$  is most accessible and affordable for the food supply chain and customers among the three tested conditions. To simulate different possible thawing situations in manufacturing and applications, thawing in a 4  $^{\circ}\text{C}$  refrigerator (T1), in ambient air (T2), or in room temperature water (T3) was performed, representing various thawing rates.

Images of F1 JICs and cross-sections of F1 JICs after one or five FT cycles, and SEM images of the lyophilized F1 JICs before and after FT treatments, are shown in Figure S1 (in the Supporting Information) and Figure 1a,b. Similar to our earlier findings,<sup>8</sup> severe damage of hydrogel matrix structures of F1 JICs after repeated F1TCs was observed. Visible cavities and defects of F1 JICs were formed after only one F1TC under all three thawing conditions (F1T1, F1T2, and F1T3). For all F1 JICs, significantly uneven surfaces with different sizes of cells were present throughout the matrix structures, while long and deep crevices were visible throughout the clusters of smaller cells. The size variations within and among each specimen were notable and random. The dominant disruption of the polymer matrix network should have been produced by the large and irregular ice grains formed at  $-20$   $^{\circ}\text{C}$ .

The resulting polymer network structures were closely connected with the shape and sizes of the ice grains formed during the freezing steps.<sup>13,18,28–31</sup> During the freezing steps, three major changes occur within JICs: (1) the initial nucleation of ice crystals from freezable water in the hydrogel, (2) the ice growth from single crystals to ice grains, and (3)



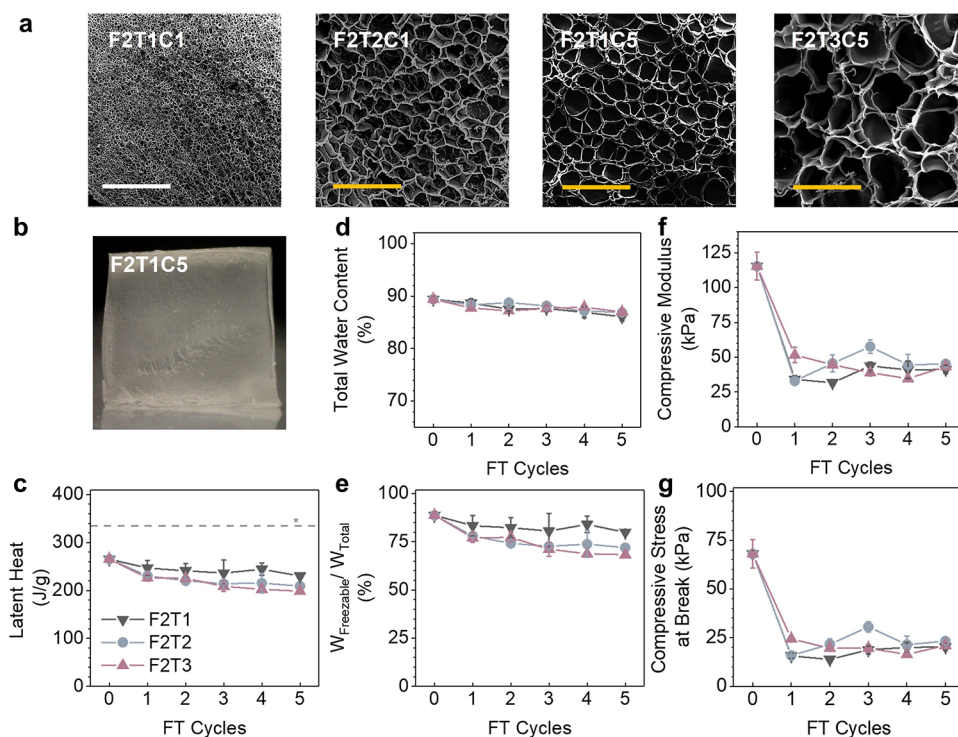


**Figure 2.** (a) SEM images of the lyophilized F2 JICs, with a white scale bar of 500  $\mu\text{m}$  and a yellow scale bar of 100  $\mu\text{m}$ . (b) Photo of the cross-section of an F2 JIC (F2T1C5). (c) Latent heat of the JICs treated under multiple F2TCs. The dashed line with a star symbol represents the latent heat value of traditional ice. (d) Changes of total water content of F2 JICs along F2TCs. (e) Freezable water to total water ratios in the F2 JICs. Static compressive modulus at break (f) and stress at break (g) of the prepared F2 JICs. Plotted data are expressed as means  $\pm$  SD of three replicates.

the segregation of polymer chains on the ice grain boundary and the formation of the macronetwork of the protein–polymer chains.<sup>31</sup> At  $-20\text{ }^{\circ}\text{C}$ , the ice formation inside the JICs is a slow process among three freezing temperature levels. Due to the low nucleation rate at  $-20\text{ }^{\circ}\text{C}$ , a small portion of cooled droplets could form the nucleus.<sup>13,18,28,31</sup> The considerable amount of freezable water molecules aggregates around the formed nucleus, and the size of the ice grains grows. Because of the mild freezing condition, the heat distribution inside the JICs during the freezing process could have caused the size distribution of the final ice grains to vary across a large scale depending on the dispersion of the nucleus. As a result, the average size of the formed ice is immense in the F1 JICs due to its lower total nucleus numbers.<sup>16,31</sup> According to Waschkie et al., the relationship between the ice-fronting velocity and the critical freezing front velocity of the system determines the final structures and positions of the polymer. At F1, the freeze-fronting velocity was slower than the critical freezing front velocity, which allowed the generation of lamellar walls and large cells of protein networks in the final scaffold.<sup>18,27</sup> The expansion of the solvent ( $\text{H}_2\text{O}$ ) volume from liquid water to solid ice encroaches the space of the solute (protein–polymer chains) and creates cells and flaws across the F1 JICs. Meanwhile, the expansion of the solvent shortens the distance of inter- and intraprotein macromolecular chains, which first significantly enlarges the possibilities of forming inter-macromolecular H-bonds, increases the degree of physical cross-linking of the polymer network, and increases the possibilities of forming disulfide bonds between sulfhydryl groups.<sup>15</sup> Once stabilized by H-bonds and disulfide bonds, the nonuniform hollow structures with many material flaws stay in F1 JICs even after the solvent (ice) thaws back to the liquid status.

Here, it is critical to identify the relationship between the morphological change and performance of JICs after repeated FT treatments. The heat-absorbing ability near  $0\text{ }^{\circ}\text{C}$  is the critical indicator of the food cooling functions. Figure 1c shows the changes of fusion heat of F1 JICs from FTC0 to F1TC5. The average latent heat of fusion at FTC0 was 265.35 J/g, and after several FT cycles, it showed an apparent decreasing tendency under all three thawing rates. For the sample of F1T1 JICs, the average fusion heat dropped by around 14% after three FT cycles and more than 20% after five FT cycles. For samples of F1T2 and F1T3, there were more than 25% decrease after three F1TCs and more than 35% decrease after five FT cycles. The latent heat of fusion of JICs around  $0\text{ }^{\circ}\text{C}$  is associated with the amount of freezable water in the hydrogel structures. Thus, the change of water contents in the structure of F1 JICs was also tested. In Figure 1d, the total water content in F1 JICs showed steady decreasing tendencies under all three thaw rates. The water loss difference induced by different thawing rates was not significant ( $P < 0.05$ ). However, it should be noted that the first three F1TCs introduced the most significant losses in total water content for all F1 JIC groups, especially for F1T3. In contrast, the water content was maintained in a steady status afterward. Figure 1e describes the percentage change of the freezable water in the total water content in F1 JICs. With very similar trends found in Figure 1f, after F1TC1, the average freezable water reduced from 88.8% (FTC0) to 81.6%, 83.8%, and 77.4% for F1T1C1, F1T2C1, and F1T3C1, respectively. Moreover, after F1TC5, the F1 JICs retained only 74.3% (F1T1C5), 60.9% (F1T2C5), and 59.6% (F1T3C5) freezable water in the total water contents. The loss of freezable water content should be closely associated with the morphological change of the polymer network structures of F1

JICs induced by FT treatments. Many large ice grains were generated at  $-20\text{ }^{\circ}\text{C}$ , making it challenging for the  $\text{H}_2\text{O}$  molecules in the middle of the ice grains to interact with the polymer chains through H-bonds due to the excessively long distance. With fewer H-bonding interactions, those  $\text{H}_2\text{O}$  molecules became unconstrained water and could be lost once thawed.

Meanwhile, as shown in Figure 1f,g, the compressive mechanical properties of F1 JICs were significantly damaged after the FT treatments due to the generated cavities and flaws described in the earlier discussions. The compressive modulus in Figure 1f shows the hardness of the JICs, while the compressive stress at break indicates the highest pressure that the hydrogels can bear. From C1 to C5, a cross-linking effect on F1 JICs induced by the FT treatments was observed with increased mechanical strength. The increase of H-bonds and the possible increase of disulfide bonds contribute to strengthening the hydrogel matrix structures in F1 JICs. However, even with the strengthening, the overall mechanical stress at break was around 10–16 kPa after F1T3C5, around 76–85% of loss compared to FTC0.

In summary, the weakening impact of ice grains formed at  $-20\text{ }^{\circ}\text{C}$  was quite impressive on the structures of F1 JICs as well as on their functions. With repeated F1TCs, the morphology of the polymer networks of the F1 JICs was significantly disrupted by various sizes of irregular ice grains. The average large cell size within the JICs reduced the possibility of freezable water interacting with the protein macromolecules, thus increasing freezable water loss in the repeated F1TCs. There was an apparent decrease in the heat-absorbing ability and a striking decrease in the mechanical properties of the F1 JICs treated with various thawing rates, though a slower thawing rate (T1) mildly lessened the performance degradation of the F1 JICs. Overall, to advance the performance and prolong the lifecycles of JICs, extra modifications should be made to stabilize the structure of the polymer network in JICs against the deformation forces of ice grains observed under the F1 condition.

**JICs Prepared in a Dry Ice–Ethanol Bath (F2 JICs).** To increase the freezing rate in the JIC preparation step, a dry ice–ethanol bath was used to create a fast-freezing environment at  $-78.5\text{ }^{\circ}\text{C}$  (F2), which generally causes less damage to the structures because of the smaller sizes of the generated ice grains.<sup>19</sup> Here, the cryogenic condition F2 was employed to provide a more rapid cooling rate than F1 to study the freezing temperature and rate on polymer network morphology and the related properties of the formed JICs. The JICs prepared under F2 conditions are referred to as F2 JICs. According to the thawing conditions,  $4\text{ }^{\circ}\text{C}$  air (T1), ambient air (T2), or room temperature water (T3), F2 JICs were labeled with F2T1, F2T2, and F2T3, respectively.

The appearances, lyophilized specimens, and the cross-sectional structures of all F2 JICs after F2TC1 or F2TC5 are shown in Figure S2 (Supporting Information) and Figure 2a,b. The impact of the phase change of water on the polymer matrix structures was controlled. Under the F2 condition, the ice freezing front velocity was higher than the critical velocity of the system, which allowed some portion of polymer macromolecules to be entrapped in the ice framework as bridges between lamellar walls and resulting in the formation of finer-scale porosity.<sup>18,28</sup> Compared to the samples of F1 JICs, specimens of F2 JICs showed much denser and more uniform structures with no large visible crack but minor

ditches, indicating a large amount of finer ice grains generated in the protein matrix structure. Moreover, various thawing rates of the F2 JICs also impacted the structures of polymer networks formed, which is illustrated by the SEM images of F2T1C5 and F2T3C5 (Figure 2a). The average cell size of the JICs after F2T3C5 treatments was much larger than that of the F2T1C5, which might be related to a higher degree of physical cross-linking of the protein network at a high thawing rate.<sup>9,17,23</sup>

Tests on the properties and functions of F2 JICs were also conducted to find if the morphology of F2 JICs with higher uniformity enables the stabilized functions and prolonged JIC lifecycles. Figure 2c shows that the latent heat of fusion of JICs after the F2T1 treatments was very stable. The average latent heat values of F2 JICs slightly decreased from 265.35 J/g (FTC0) to 246.89 J/g at F2T1C1. After F2T1C5, the average latent heat of fusion of JICs only dropped by 13%, which was much less than any of the F1 JICs. Meanwhile, the slowest thawing rate, T1, also showed the best performance in maintaining the structural stability and heat-absorbing ability of the F2 JICs among all thawing conditions. The average fusion heat of JICs after F2T2C1 and F2T3C1 dropped by 13% and 15%, respectively, compared to that of the FTC0. After five cycles of FT treatments, the F2 JICs of F2T2C5 and F2T3C5 still retained fusion heat values of 209.17 and 198.57 J/g, which were much higher than those of F1T2C5 and F1T3C5. Apparently, the lower freezing temperature and higher freezing rate stabilized the heat-absorbing abilities of JICs, and a slower thawing rate reduced the loss of fusion heat around  $0\text{ }^{\circ}\text{C}$ , better than a faster thawing rate. A similar pattern was observed in the change of total water content and freezable water ratio of JICs, as shown in Figure 2d,e. The overall changes in the total water content of F2 JICs were not quite significant as compared to those of F1 JICs. After F2TC1, F2 JICs of F2T1C1, F2T2C1, and F2T3C1 showed an average of 88.7%, 88.3%, and 87.8% of total water contents, respectively. After F2TC5, 86.1% (F2T1C5), 86.9% (F2T2C5), and 87.0% (F2T3C5) of total water remained in JICs, which were higher than all of the F1 JICs after F1TC5. The freezable water content was also maintained stably under the F2T1 treatment. After F2T1C5, there was only an 8% drop in the ratio of freezable water over the total water content. For JICs after F2T2C5 and F2T3C5, the ratio dropped by 16% and 17% compared to FTC0 but was still much less than F1 JICs after F1T2C5 and F1T3C5. By incorporating a lower temperature bath and a faster freezing rate, the heat-absorbing ability of JICs along multiple F2TCs was improved with much less water loss, especially on the freezable water content, from the hydrogel structures.

Figure 2f,g shows the compressive modulus and compressive stress at break of the F2 JICs. Similar to what was observed in the F1 series, the modulus of F2 JICs dropped sharply after F2TC1 under all thawing conditions (F2T1C1, F2T2C1, and F2T3C1). When treated with the F2T3 condition, the modulus showed a continuous decreasing tendency along five FT cycles, while the F2T1 JICs showed an increasing trend from F2T1C2 to F2T1C5, which were also similar to what was observed with F1 JICs. However, the overall loss of mechanical strength of F2 JICs due to the repeated FT cycles was not as significant as those treated under the F1 condition. After F2TC5, the average compressive stress at break for all F2 JICs was higher than 20 kPa, which doubled the stress of the JICs

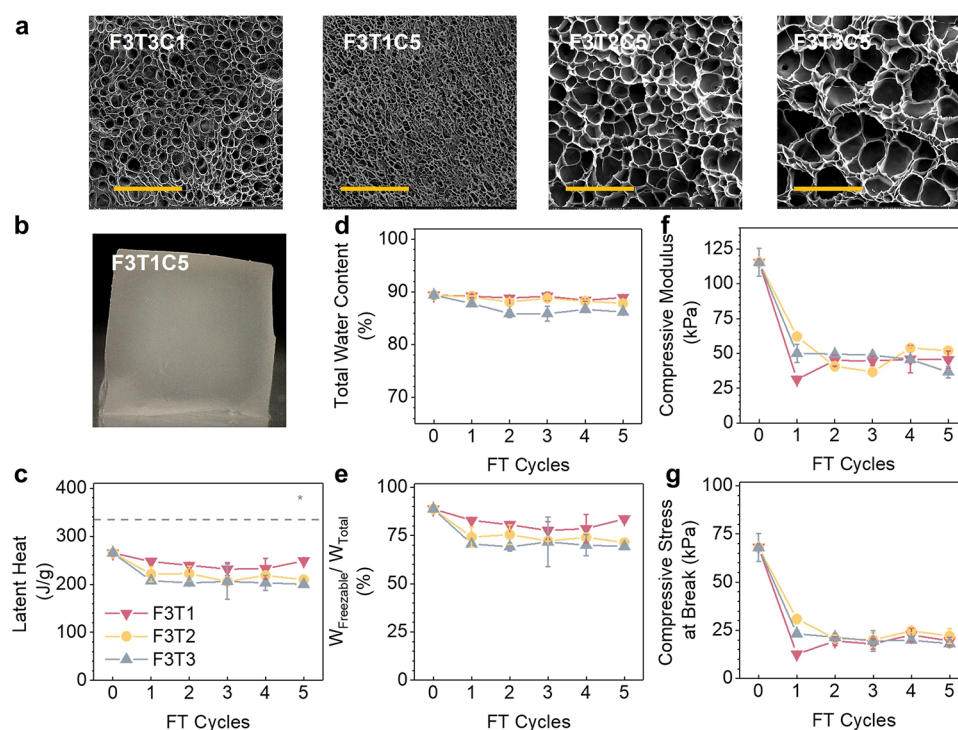


**Figure 3.** (a) SEM images of the lyophilized F3 JICs, with a white scale bar of 500  $\mu\text{m}$  and a yellow scale bar of 100  $\mu\text{m}$ . (b) Photo of the cross-section of an F3 JIC (F3T1C5). (c) Latent heat of the JICs treated under multiple F3T Cs. The dashed line with a star symbol represents the latent heat value of traditional ice. (d) Changes of total water content of F3 JICs along F3T Cs. (e) Freezable water to total water ratios in the F3 JICs. Static compressive modulus at break (f) and stress at break (g) of the prepared F3 JICs. Plotted data are expressed as means  $\pm$  SD of three replicates.

treated with F1T C5 and met beyond the required 10 kPa strength limit for over 10 m of overhead food load.<sup>8</sup>

Overall, the F2 rapid freezing cycles significantly reduced the morphological disruption of the JICs by ice grains compared to those under the F1 condition. The uniform and fine porous morphology of the F2 JICs structures improved the freezable water content and, consequently, the compressive mechanical stability.

**JICs Prepared in a Liquid Nitrogen Bath (F3 JICs).** To continue exploring the possible advantages of rapid freezing rate and lower temperature on the structural features and cooling performance of JICs in the repeated FT cycles, a cryogenic condition at  $-198\text{ }^{\circ}\text{C}$  provided with a liquid nitrogen bath was used in this section as the F3 series. All three thawing conditions of T1, T2, and T3 were employed on F3 JICs as well.

Figure 3a,b and Figure S3 (Supporting Information) together show the appearances, cross-sectional images of the F3 JICs after varied thawing and freezing cycles, as well as the lyophilized specimens. Multiple changes were observed from F3 JIC specimens compared to those from the F1 JICs and F2 JICs. First, the overall structures became opaque (Figure 3b), indicating that more polymer crystalline domains formed during F3T1 treatment. Second, the overall hydrogel structure remained intact, with tiny cracks caused by the phase change of water. Most importantly, the cell size of the F3 JICs after F3T1C5 was intensively smaller than the specimens after F1T1C5 and F2T1C5, which was because of the high ice-fronting velocity during F3 freezing steps.<sup>18,28</sup> The observed phenomena also agree with what was found by Bodenberger et al.<sup>32</sup> Since JICs at FTC0 were of homogeneous status,<sup>8</sup> it is fair to say that F3T1 preserved the original morphology of the JICs

to the best degree among all of the tested FT conditions via refined solidification of water.

Similar to the F2 series, the changes of latent heat of fusion of F3 JICs, shown in Figure 3c, were very steady compared to those of F1 JICs. The average latent heat of fusion was around 248.8, 209.7, and 199.9 J/g for the samples of F3T1C5, F3T2C5, and F3T3C5, respectively. The total water contents in Figure 3d show that, compared to FTC0 gels, JICs treated under F3T1 and F3T2 did not lose a significant amount of water in five cycles ( $P < 0.05$ ). The JICs treated under the F3T3 condition, however, showed slight total water losses. Also, in Figure 3e, the ratios of freezable water in the total water content revealed that F3T1 gels maintained the highest freezable water content in the structure, whereas F3T3 maintained the least. With the results obtained from F1 and F2 JICs, it can be concluded that the slowest thawing rate, T1, preserved the highest portion of the freezable water content in the hydrogel structure, contributing to the best-preserved heat-absorbing abilities of JICs near  $0\text{ }^{\circ}\text{C}$ .

Again, the mechanical properties of F3 JICs shown in Figure 3f,g illustrate that an even more rapid freezing rate further reduced the damage of ice grains to the polymer network in the JICs, compared to F2 JICs. Agreed with what was seen in the SEM images, the structure of the F3 JICs after repeated FT cycles had much fewer flaws compared to the F1 and F2 JICs undergoing the same cycles of treatments, with the average compressive modulus staying at 46, 52, and 37 kPa for samples of F3T1C5, F3T2C5, and F3T3C5, respectively. After F3T C5, the average compressive stress at break was around 20 kPa for the F3 JICs.

In summary, the F3 treatment preserved the best of the morphologies of JICs in the repeated phase-change cycles



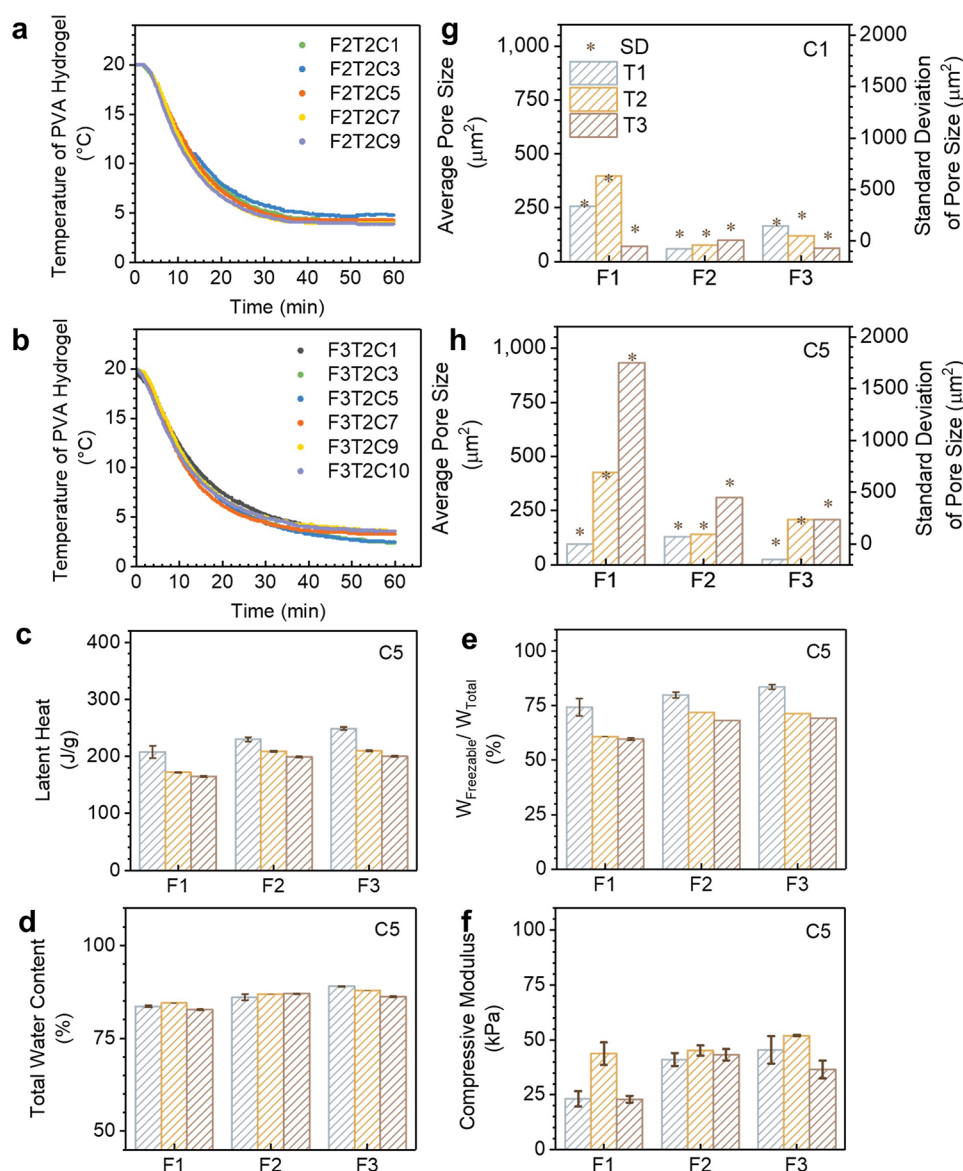


**Figure 4.** Overall comparison of F1, F2, and F3 JICs. Cooling curves of JICs in multiple use cycles under F2T2 (a) and F3T2 (b). Comparison of latent heat (c), total water content (d), freezable water content (e), and compressive modulus (f) of F1, F2, and F3 JICs after FTCS. Average pore size and variation of lyophilized JICs after FTC1 (g) and FTC5 (h).

among all three levels of freezing temperatures, and the F3T1 treatment generated the most uniform structures with tiny microcells among all F3 JICs. In good agreement with the morphology characteristics, the freezable water content of F3T1 gels was maintained in a pretty stable status through five FT cycles, as were the heat-absorbing abilities during the uses. The decline of the gel strength through repeated use cycles was well-controlled and reduced compared to the JICs prepared in a conventional freezer (F1 JICs).

**Analysis of Structure and Performance of JICs.** For a more intuitive comparison, the properties of F1, F2, and F3 JICs are presented in Figure 4. First, as demonstrated in the earlier study, cooling curves of JICs toward food subjects (simulated by PVA/RBPS hydrogels) were compared under room temperature air (T2).<sup>8</sup> In the previous study, the cooling efficiency of F1 JICs was found with a noticeable decrease, where the final temperature of cooling objects increased from 4.4 °C (cooled by JICs at F1T2C1) to 5.1 °C (cooled by JICs at F1T2C5). In comparison, as shown in Figure 4a,b, when

JICs were used under F2T2 or F3T2 conditions, there was no apparent change in the final temperature of the cooled object even after 9 or 10 FT cycles. After 60 min of cooling with the F2 JICs, the temperature of the cooled object remained in the range  $4.0 \pm 0.3$  °C within the nine cycles of repeated applications. When cooled with the F3 JICs, the final temperatures of the cooled objects were always below 3.6 °C along with 10 application cycles. The results of the cooling efficiency agreed well with the structural features discussed earlier that JICs frozen under a lower temperature present a higher stability in heat-absorbing abilities.

In addition, Figure 4c–f directly compares the latent heat, total water content, freezable water content, and compressive modulus of JIC after F1TCS, F2TCS, and F3TCS. After five cycles of thawing and freezing, the impact of the freezing temperature and thawing conditions on the performance of the JICs was amplified and distinct. It can be observed that the overall tendencies of latent heat of fusion, total water content, and freezable water content were very similar. The effect of the

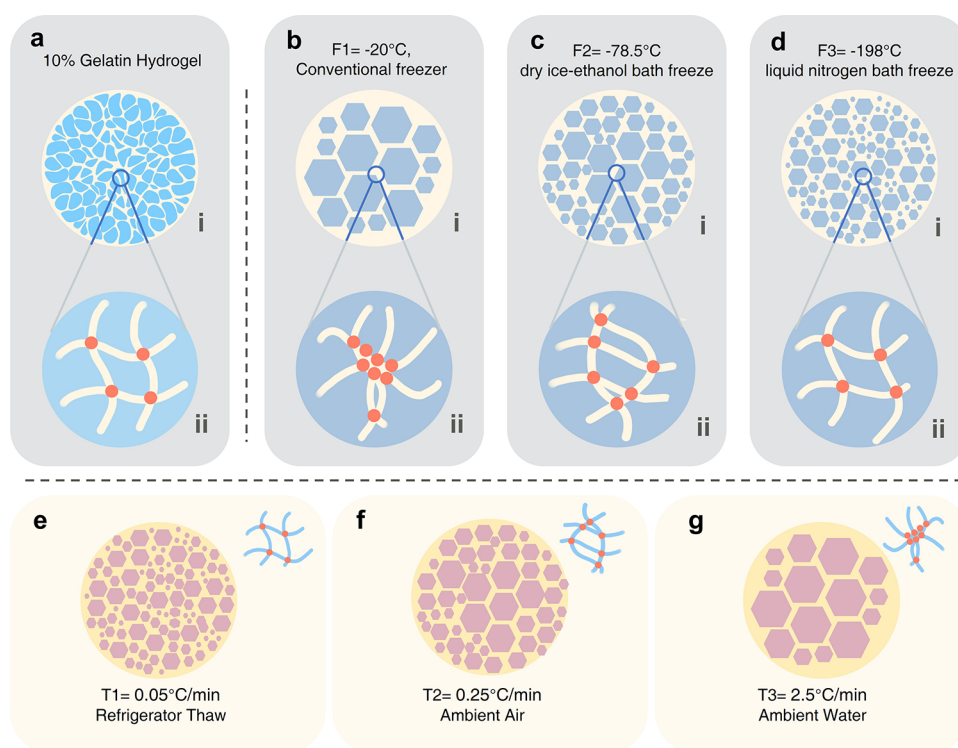


**Figure 5.** Schematic drawing on the freeze–thaw effect to the structures of JICs under different FT conditions. (a) 10% gelatin hydrogels under room temperature before FT treatments. JICs frozen at  $-20^{\circ}\text{C}$  (b),  $-78.5^{\circ}\text{C}$  (c), and  $-198^{\circ}\text{C}$  (d). JICs thawed at  $-20^{\circ}\text{C}$  (e),  $-78.5^{\circ}\text{C}$  (f), and  $-198^{\circ}\text{C}$  (g). The water and ice fractions are shown in either blue (fresh or frozen, a–d) or pink (thawed, e–g). The portion of protein polymers is shown in either ivory (a–d) or yellow (e–g). Orange dots represent the possible cross-linking spots within the polymer network. The status of polymer macronetworks under a thawed status is also shown in the top right corner in blue with orange cross-linking spots in parts e–g.

low-temperature rapid freezing technique was evident in increasing the stability and durability of the JICs. Under the same thawing condition, F3 JICs retained the best performance among gels along with five cycles by showing the highest latent heat of fusion, highest total water content, highest freezable water content, and highest mechanical strength. Meanwhile, a slower thawing rate also contributed to stabilizing the performance of JICs and reducing the destructive impact of repeated FT cycles. Under the same freezing condition, T1 reliably provides the highest heat-absorbing ability and freezable water content.

Since the features of the polymer macronetworks of JICs are closely connected to the size and shapes of the formed ice grains under a frozen status,<sup>31</sup> the average pore size and pore size variation of the lyophilized JICs were controlled by the cooling temperature–freezing rate, as well as the thawing rate. Finer and well-controlled porous structures of JICs could improve the retention of total and freezable water in the hydrogels and the mechanical performance of JICs. Figures 4g,h and 5 together illustrate the effect of various freeze–thaw conditions on the inner structures of JICs by showing the obtained data and highlighting the observed phenomena schematically, respectively. After FTC1, as shown in Figure 4g, though the difference among groups was not explicit enough after only FTC1, it can be observed that the F1 JICs generated larger pore sizes with a broader variation. After FTC5, as shown in Figure 4h, the pore sizes of JICs generated under different freezing temperatures and thawing rates vary compellingly. With F1, the average pore sizes of F1 JICs became  $95.60 \pm 121.11$ ,  $425.58 \pm 664.90$ , and  $933.30 \pm 1800.69 \mu\text{m}^2$  for F1T1C5, F1T2C5, and F1T3C5 samples,

respectively. The F2 JICs revealed relatively smaller (except for F2T1) pore sizes of  $129.87 \pm 177.01$ ,  $139.37 \pm 174.96$ , and  $309.48 \pm 591.05 \mu\text{m}^2$  after F2T1C5, F2T2C5, and F2T3C5, respectively. The F3 JICs demonstrated all smaller pore sizes at  $23.72 \pm 20.61$ ,  $208.63 \pm 227.27$ , and  $207.37 \pm 390.39 \mu\text{m}^2$  for F3T1C5, F3T2C5, and F3T3C5, respectively.

On one hand, from the obtained data, a pattern was found that a lower freezing temperature and slower thawing rate significantly reduced the average pore size with a narrower size distribution, which is schematically highlighted in Figure 5. In Figure 5a–d, the status of both ice grains and polymer macronetworks in a frozen JIC is described, where part i focuses on the status of ice grains in JICs, and part ii enlarges the status of polymer networks and the possible cross-linking spots. With F1 freezing conditions, the slow initial nucleation rate resulted in the large aggregation of ice grains, where the water solidification front velocity was slower than the critical freezing front velocity.<sup>18,31</sup> The expelled protein polymers due to the solidification of solvent generated polymer macronetworks with large and irregular cells with significant size variations (Figure 5b). When the freezing temperature was reduced to F2 or F3, as shown in Figure 5c,d, the ice-fronting velocity was higher than the critical velocity, yielding finer-scale porosity throughout the structure of the frozen JICs, with around 1/2 to 1/30 pore size of the F1 JICs. Figure 5e–g demonstrates that slow thawing conditions are less effective to the physical cross-linking of the protein caused by H-bonds and reduce the disruption of the original 3D networks in JICs caused by the water phase change. In general, a slower thawing rate resulted in the finer and stabler structure of JICs via a slower phase change of the solvent. The impact of the thawing process was



also based on the structures formed during the freezing steps of the FT treatment. The impact on the gel polymer structure from both the freezing and thawing process could be permanent as long as the status of the protein network was not alternated by high temperatures or other extreme conditions.

On the other hand, water–protein interactions in the original homogeneous hydrogel systems were altered by the solidification and melting of water. The rapid freezing and slow thawing process decreased the loss of water content with the slightest degree of physical cross-linking within the protein–polymer network. By minimizing the formation of H-bonds and disulfide bonds within the protein macronetwork, JICs treated with F3T1 maintain the total water content and freezable water content at a similar level of the fresh JICs (F0 JICs), preserving the hydrophilicity of the materials, which guarantees the cooling ability of JICs along 10 or more application cycles. Also, due to the slightest structural changes of F3T1 JICs, the mechanical stability of JICs was also improved and maintained above the required 10 kPa level for up to 10 m of overhead food load.<sup>8</sup>

## CONCLUSIONS

JICs, as a type of new reusable and green cooling medium, should possess robust properties against the phase change of the water in the hydrogel matrix materials and provide consistent cooling functions during repeated uses. From the earlier study, the significant influence of ice grains formed during the FT treatments in the structure and function of JICs was noticed. In this study, various FT conditions have been systematically investigated to produce a fine protein–polymer network by controlling the ice grain formation and fusion conditions. The combination of rapid freezing and slow thawing treatment conditions generated uniform polymer network structures after multiple FT cycles. Under the conditions of a liquid-nitrogen bath and the slowest rate thawing (F3T1), JICs still possess optimized fine inner structures (pore size =  $23.72 \pm 20.61 \mu\text{m}^2$ ) with the stable latent heat of fusion (248.8 J/g), constant total water content (around 90%) and cooling efficiency, and relatively stable mechanical strength (46 kPa) after F3T1C5. The stable cooling efficiency of F3 JICs was retained for up to 10 repeated usage cycles. The found pattern in the effect of freezing and thawing conditions on the structures and properties of hydrogels agreed with earlier studies and could guide the fabrication and application condition of JICs and other water-rich systems. However, it should be noted that rapid freeze conditions of using liquid nitrogen or dry ice and anhydrous ethanol in the preparation of JICs might be only practical to commercial users and out of reach to regular customers. A more convenient application procedure should be investigated for the practical use of such novel cooling materials.

## ASSOCIATED CONTENT

### Supporting Information

The Supporting Information is available free of charge at <https://pubs.acs.org/doi/10.1021/acssuschemeng.1c06309>.

Photos and SEM images of F1 JICs treated with  $-20\text{ }^\circ\text{C}$  freezing (F1) and three thaw conditions, photos and SEM images of F2 JICs treated with  $-78\text{ }^\circ\text{C}$  freezing (F2) and three thaw conditions, and photos and SEM

images of F3 JICs treated with  $-198\text{ }^\circ\text{C}$  freezing (F3) and three thaw conditions (PDF)

## AUTHOR INFORMATION

### Corresponding Author

Gang Sun – Department of Biological and Agricultural Engineering, University of California, Davis, California 95616, United States; [orcid.org/0000-0002-6608-9971](https://orcid.org/0000-0002-6608-9971); Phone: (530) 752-0840; Email: [gysun@ucdavis.edu](mailto:gysun@ucdavis.edu)

### Authors

Jiahua Zou – Department of Biological and Agricultural Engineering, University of California, Davis, California 95616, United States; [orcid.org/0000-0001-8250-7670](https://orcid.org/0000-0001-8250-7670)

Luxin Wang – Department of Food Science and Technology, University of California, Davis, California 95616, United States

Complete contact information is available at: <https://pubs.acs.org/10.1021/acssuschemeng.1c06309>

### Notes

The authors declare no competing financial interest.

## ACKNOWLEDGMENTS

This project is financially supported by the USDA-NIFA grant 2020-67017-31275. The authors are also grateful for the Henry A. Jastro Graduate Research Award. The Thermo Fisher Quattro ESEM was funded through the US National Science Foundation under award DMR-1725618.

## REFERENCES

- (1) Adamashvili, N.; Chiara, F.; Fiore, M. Food Loss and Waste, a Global Responsibility?! *Econ Agro-alimentare* **2020**, No. 3, 825–846.
- (2) Wang, Y.; Yuan, Z. Enhancing Food Security and Environmental Sustainability: A Critical Review of Food Loss and Waste Management. *Resour Environ. Sustain* **2021**, *4*, 100023.
- (3) Karunasagar, I.; Karunasagar, I. Challenges of Food Security – Need for Interdisciplinary Collaboration. *Procedia Food Sci.* **2016**, *6*, 31–33.
- (4) Shafiee-Jood, M.; Cai, X. Reducing Food Loss and Waste to Enhance Food Security and Environmental Sustainability. *Environ. Sci. Technol.* **2016**, *50* (16), 8432–8443.
- (5) Ndraha, N.; Hsiao, H. I.; Vljajic, J.; Yang, M. F.; Lin, H. T. V. Time-temperature abuse in the food cold chain: Review of issues, challenges, and recommendations. *Food Control* **2018**, *89*, 12.
- (6) Schirone, M.; Visciano, P.; Tofalo, R.; Suzzi, G. Editorial: Biological Hazards in Food. *Front. Microbiol.* **2017**, *7*, 2154.
- (7) UCDA danger Zone. [https://www.fsis.usda.gov/wps/portal/ffis/topics/food-safety-education/get-answers/food-safety-fact-sheets/safe-food-handling/danger-zone-40-f-140-f/CT\\_Index](https://www.fsis.usda.gov/wps/portal/ffis/topics/food-safety-education/get-answers/food-safety-fact-sheets/safe-food-handling/danger-zone-40-f-140-f/CT_Index) (accessed March 2021).
- (8) Zou, J.; Wang, L.; Sun, G. Sustainable and Reusable Gelatin-based Hydrogel “Jelly Ice Cubes” as Food Coolant. I: Feasibilities and Challenges. *ACS Sustainable Chem. Eng.* **2021**, XXXX (XXX), XXX–XXX.
- (9) Lin, T.; Wang, J. J.; Li, J. B.; Liao, C.; Pan, Y. J.; Zhao, Y. Use of Acidic Electrolyzed Water Ice for Preserving the Quality of Shrimp. *J. Agric. Food Chem.* **2013**, *61*, 8695–8702.
- (10) Wang, J. J.; Lin, T.; Li, J. B.; Liao, C.; Pan, Y. J.; Zhao, Y. Effect of Acidic Electrolyzed Water Ice on Quality of Shrimp in Dark Condition. *Food Control* **2014**, *35* (1), 207–212.
- (11) Zhao, L.; Zhang, Z.; Wang, M.; Sun, J.; Li, H.; Malakar, P. K.; Liu, H.; Pan, Y.; Zhao, Y. New Insights into the Changes of the Proteome and Microbiome of Shrimp (*Litopenaeus Vannamei*)

Stored in Acidic Electrolyzed Water Ice. *J. Agric. Food Chem.* **2018**, *66*, 4966–4976.

(12) Shin, J.-H.; Chang, S.; Kang, D.-H. Application of Antimicrobial Ice for Reduction of Foodborne Pathogens (*Escherichia Coli* O157:H7, *Salmonella* Typhimurium, *Listeria Monocytogenes*) on the Surface of Fish. *J. Appl. Microbiol.* **2004**, *97* (5), 916–922.

(13) Lozinsky, V. I.; Galaev, I. Yu.; Plieva, F. M.; Savina, I. N.; Jungvid, H.; Mattiasson, B. Polymeric Cryogels as Promising Materials of Biotechnological Interest. *Trends Biotechnol.* **2003**, *21* (10), 445–451.

(14) Lozinsky, V. I. Cryostructuring of Polymeric Systems. 55. Retrospective View on the More than 40 Years of Studies Performed in the A.N.Nesmeyanov Institute of Organoelement Compounds with Respect of the Cryostructuring Processes in Polymeric Systems. *Gels* **2020**, *6* (3), 29.

(15) Okay, O., Ed. *Polymeric Cryogels, Macroporous Gels with Remarkable Properties*; Springer, 2014. DOI: 10.1007/978-3-319-05846-7.

(16) Ickes, L.; Welti, A.; Hoose, C.; Lohmann, U. Classical Nucleation Theory of Homogeneous Freezing of Water: Thermodynamic and Kinetic Parameters. *Phys. Chem. Chem. Phys.* **2015**, *17* (8), 5514–5537.

(17) Li, B.; Sun, D.-W. Novel Methods for Rapid Freezing and Thawing of Foods – a Review. *J. Food Eng.* **2002**, *54* (3), 175–182.

(18) Shao, G.; Hanaor, D. A. H.; Shen, X.; Gurlo, A. Freeze Casting: From Low-Dimensional Building Blocks to Aligned Porous Structures—A Review of Novel Materials, Methods, and Applications. *Adv. Mater.* **2020**, *32* (17), 1907176.

(19) William, S. The science of freezing foods. *University of Minnesota Extension*, 2018. <https://extension.umn.edu/preserving-and-preparing/science-freezing-foods> (accessed April 2021).

(20) Petzold, G.; Aguilera, J. M. Ice Morphology: Fundamentals and Technological Applications in Foods. *Food Biophys* **2009**, *4* (4), 378–396.

(21) Tan, M.; Lin, Z.; Zu, Y.; Zhu, B.; Cheng, S. Effect of Multiple Freeze-Thaw Cycles on the Quality of Instant Sea Cucumber: Emphatically on Water Status of by LF-NMR and MRI. *Food Res. Int.* **2018**, *109*, 65–71.

(22) Li, D.; Zhu, Z.; Sun, D.-W. Effects of Freezing on Cell Structure of Fresh Cellular Food Materials: A Review. *Trends Food Sci. Technol.* **2018**, *75*, 46–55.

(23) Boonsumrej, S.; Chaiwanichsiri, S.; Tantratian, S.; Suzuki, T.; Takai, R. Effects of Freezing and Thawing on the Quality Changes of Tiger Shrimp (*Penaeus Monodon*) Frozen by Air-Blast and Cryogenic Freezing. *J. Food Eng.* **2007**, *80* (1), 292–299.

(24) Zhang, M.; Li, F.; Diao, X.; Kong, B.; Xia, X. Moisture Migration, Microstructure Damage and Protein Structure Changes in Porcine Longissimus Muscle as Influenced by Multiple Freeze-Thaw Cycles. *Meat Sci.* **2017**, *133*, 10–18.

(25) Tan, M.; Mei, J.; Xie, J. The Formation and Control of Ice Crystal and Its Impact on the Quality of Frozen Aquatic Products: A Review. *Crystals* **2021**, *11* (1), 68.

(26) Lozinsky, V. I. Cryostructuring of Polymeric Systems. 50. Cryogels and Cryotropic Gel-Formation: Terms and Definitions. *Gels (Basel, Switzerland)* **2018**, *4* (3), 77.

(27) Qin, H.; Zhang, Y.; Jiang, J.; Wang, L.; Song, M.; Bi, R.; Zhu, P.; Jiang, F. Multifunctional Superelastic Cellulose Nanofibrils Aerogel by Dual Ice-Templating Assembly. *Adv. Funct. Mater.* **2021**, 2106269.

(28) Waschkes, T.; Oberacker, R.; Hoffmann, M. J. Investigation of Structure Formation during Freeze-Casting from Very Slow to Very Fast Solidification Velocities. *Acta Mater.* **2011**, *59* (13), 5135–5145.

(29) Deville, S. The Lure of Ice-Templating: Recent Trends and Opportunities for Porous Materials. *Scr. Mater.* **2018**, *147*, 119–124.

(30) Deville, S. Ice-Templating, Freeze Casting: Beyond Materials Processing. *J. Mater. Res.* **2013**, *28* (17), 2202–2219.

(31) Grenier, J.; Duval, H.; Barou, F.; Lv, P.; David, B.; Letourneur, D. Mechanisms of Pore Formation in Hydrogel Scaffolds Textured by Freeze-Drying. *Acta Biomater.* **2019**, *94*, 195–203.

(32) Bodenberger, N.; Kubiczek, D.; Abrosimova, I.; Scharm, A.; Kipper, F.; Walther, P.; Rosenau, F. Evaluation of Methods for Pore Generation and Their Influence on Physio-Chemical Properties of a Protein Based Hydrogel. *Biotechnology Reports* **2016**, *12*, 6–12.